

Evaluation of carbonic anhydrase and paraoxonase inhibition activities and molecular docking studies of highly water-soluble sulfonated phthalocyanines

Emre GÜZEL^{1*}, Fatih SÖNMEZ², Sultan ERKAN³, Kübra ÇIKRIKÇI⁴,
Adem ERGÜN⁴, Nahit GENÇER⁴, Oktay ARSLAN⁴, Makbule B. KOÇAK⁵

¹Department of Fundamental Sciences, Faculty of Technology, Sakarya University of Applied Sciences, Sakarya, Turkey

²Pamukova Vocational School, Sakarya University of Applied Sciences, Sakarya, Turkey

³Chemistry and Chemical Processing Technologies, Yıldızeli Vocational School, Sivas Cumhuriyet University, Sivas, Turkey

⁴Department of Chemistry, Faculty of Arts and Science, Balıkesir University, Balıkesir, Turkey

⁵Department of Chemistry, Faculty of Arts and Science, İstanbul Technical University, İstanbul, Turkey

Received: 09.07.2020 • Accepted/Published Online: 22.09.2020 • Final Version: 16.12.2020

Abstract: The investigation of carbonic anhydrase and paraoxonase enzyme inhibition properties of water-soluble zinc and gallium phthalocyanine complexes (**1** and **2**) are reported for the first time. The binding of p-sulfonylphenoxy moieties to the phthalocyanine structure favors excellent solubilities in water, as well as providing an inhibition effect on carbonic anhydrase (CA) I and II isoenzymes and paraoxonase (PON1) enzyme. According to biological activity results, both complexes inhibited hCA I, hCA II, and PON1. Whereas **1** and **2** showed moderate hCA I and hCA II (off-target cytosolic isoforms) inhibitory activity (K_i values of 26.09 μM and 43.11 μM for hCA I and 30.95 μM and 33.19 μM for hCA II, respectively), they exhibited strong PON1 (associated with high-density lipoprotein [HDL]) inhibitory activity (K_i values of 0.37 μM and 0.27 μM , respectively). The inhibition kinetics were analyzed by Lineweaver–Burk double reciprocal plots. It revealed that **1** and **2** were noncompetitive inhibitors against PON1, hCA I, and hCA II. These complexes can be more advantageous than other synthetic CA and PON inhibitors due to their water solubility. Docking studies were carried out to examine the interactions between hCA I, hCA II, and PON1 inhibitors and metal complexes at a molecular level and to predict binding energies.

Key words: Phthalocyanine, sulfonated, water-soluble, paraoxonase, carbonic anhydrase, enzyme inhibition, molecular docking

1. Introduction

Phthalocyanines (Pcs), an important family of porphyrinoid complexes, have many applications such as gas sensors [1], solar cells [2], liquid crystals phases [3,4], electrochromic materials [5], and photosensitizer [6–9] in photodynamic therapy (PDT). For these applications, the photophysical and photochemical features of phthalocyanines can be fine-tuned by the introduction of various substituent groups. It is also known that the physical and chemical properties of the complex depend significantly on the nature of the metal atom coordinated to the phthalocyanine ring [8,10,11]. The lack of water solubility of phthalocyanines limits their use in many areas. Also, water solubility is very important for cancer treatments because the complexes are injected into the patient's bloodstream with a hydrophilic system [12]. Water-soluble phthalocyanines continue to attract attention to their interactions with DNA and their ability to trigger DNA photodamage by accumulating in many cancer cells. Sulfonate, carboxylate, and phosphorus groups can be used from anionic substituents to the macrocyclic ring by various intermediates or directly attached to the phthalocyanine complexes. In particular, the binding of sulfonic acid groups to the phthalocyanine ring has two important effects: they increase the effectiveness of their antitumor properties [13], and by inducing the repulsion of phthalocyanine rings, they become water-soluble as monomers [9,12,14]. Also, in the literature, gallium and zinc metal complexes of the phthalocyanines are examined due to their superior antitumor properties [13]. Thus, these phthalocyanines are beneficial to PDT and various biological applications.

Carbonic anhydrase (CA) isoenzymes are metalloenzymes that catalyze a very easy reaction: the hydration of CO_2 to bicarbonate and H^+ [15–17]. This key reaction plays a significant role in more pathological and physiological mechanisms associated with ion transport, pH control, and fluid secretion [18]. The inhibition of these isoenzymes is the main goal

* Correspondence: eguzel@subu.edu.tr

correlated with the treatment of diverse diseases such as obesity, glaucoma, and epilepsy. More recently, CA inhibition was validated as a novel approach to fighting metastases and tumors. Paraoxonase, which has an important role in living metabolism, is a calcium-dependent enzyme and is also an organophosphate hydrolyzer. These enzymes can hydrolyze aromatic carboxyl esters such as phenylacetate and various lactones. The name “PON” is derived from paraoxon, a common in vitro substrate. Paraoxonase 1 (PON1), which is associated with high-density lipoprotein (HDL) with 355 amino acids, is the most studied member of the mammalian enzyme family. PON1 is considered an important enzyme for two main reasons in metabolism: (i) it protects the system against the neurotoxicity of organophosphates and (ii) oxidizing lipid levels interfere with the onset of atherosclerosis, thus preventing oxidation of low-density lipoproteins, so the activity of PON 1 is considered a risk for atherosclerosis.

Taking these properties into consideration, we focused on water-soluble complexes as a strategy to explain Pcs in conjunction with the sulfonic acid group to study enzyme inhibition, chemical interactions, and theoretical properties. In this regard, water-soluble sulfonated zinc and gallium phthalocyanine complexes (**1** and **2**) were synthesized and their inhibition potential of hCA I and II isoenzymes and paraoxonase enzyme were investigated to give direction for further studies. Also, metal effects on carbonic anhydrase and paraoxonase inhibition activity were examined. To the best of our knowledge, even though there are some studies in the literature in which phthalocyanines are evaluated as carbonic anhydrase and α -glucosidase enzyme inhibitors [19–22], carbonic anhydrase and paraoxonase inhibition activity of anionic water-soluble phthalocyanines has not been reported. Consequently, this is the first study including the evaluation of anionic water-soluble phthalocyanines bearing Ga and Zn metals and the sulfonic acid group as both potential carbonic anhydrase and paraoxonase enzyme inhibitors. Furthermore, molecular docking studies were also applied for a better understanding of the structural and binding profiles of synthesized complexes at the active sites of target enzymes.

2. Experimental design

Details on equipment, materials, enzyme inhibition, and molecular docking parameters are supplied as Supporting Information. Water-soluble zinc and gallium phthalocyanine complexes (**1** and **2**) were prepared according to the reported procedure [14,23]. Biological activity assays and IC_{50} graphs are provided in Supporting Information.

3. Results and discussion

Figure 1 shows the molecular structure of nonperipherally substituted sulfonated zinc and gallium phthalocyanine complexes (**1** and **2**).

The solution spectra show a spectral characteristic indicating D_{4h} symmetry, which is typical for Pc complexes [24]. The absorption peak in the near-UV region is the B-band or Soret band that is attributed to the $\alpha_{2u} \rightarrow e_g^*$ transition; a further band in the visible region is related to the Q-band caused by the $\pi-\pi^*$ transition $\alpha_{1u} \rightarrow e_g^*$. It can be stated that there are some vibrational bands at relatively shorter wavelengths that are a standard property of metallophthalocyanines [25]. The UV-vis absorption spectra of nonperipherally substituted phthalocyanine complexes in DMSO shows two main peaks, the characteristic ligand centered $\pi-\pi^*$ transitions of a monomeric zinc and gallium phthalocyanine derivatives (**1** and **2**) with Q-band maxima at 695 and 711 nm, respectively (Figure 2) [14,23,26].

The CA I and CA II inhibitory activities of the synthesized complexes were determined by hydratase activity (used carbon dioxide as a substrate) and esterase activity (used 4-nitrophenyl-acetate [NPA] as a substrate) assays to calculate

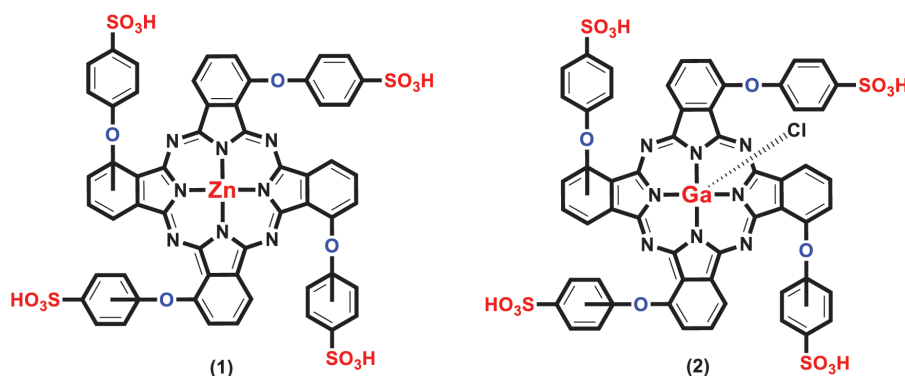


Figure 1. Molecular structure of water-soluble sulfonated zinc and gallium phthalocyanine complexes.

the inhibition constants (K_i). K_i values were calculated from the Lineweaver–Burk graphs (Figure 3). The K_i values of the synthesized compounds **1–2** against PON1, hCA I, and hCA II isoforms are given in Table 1. Complexes **1** and **2** inhibited the cytosolic isoforms hCA I and hCA II in the micromolar range (K_i values of 26.09 μM and 43.11 μM for hCA I and 30.95 μM and 33.19 μM for hCA II, respectively). Complex **1**, which included Zn metal, had higher inhibitory activity against both hCA I and hCA II with the K_i of 26.09 μM and 30.95 μM , respectively than complex **2** containing Ga metal (K_i values of 43.11 μM against hCA I and 33.19 μM against hCA II). According to these results, it could be considered that

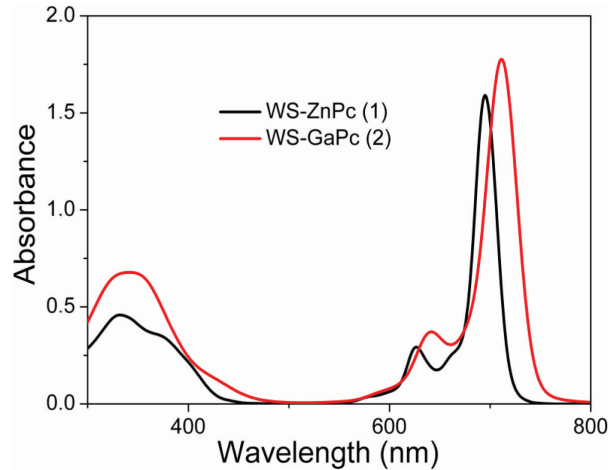


Figure 2. Absorption spectra of water-soluble zinc and gallium phthalocyanine complexes (**1** and **2**) in DMSO ($\sim 10 \times 10^{-6}$ mol dm $^{-3}$).

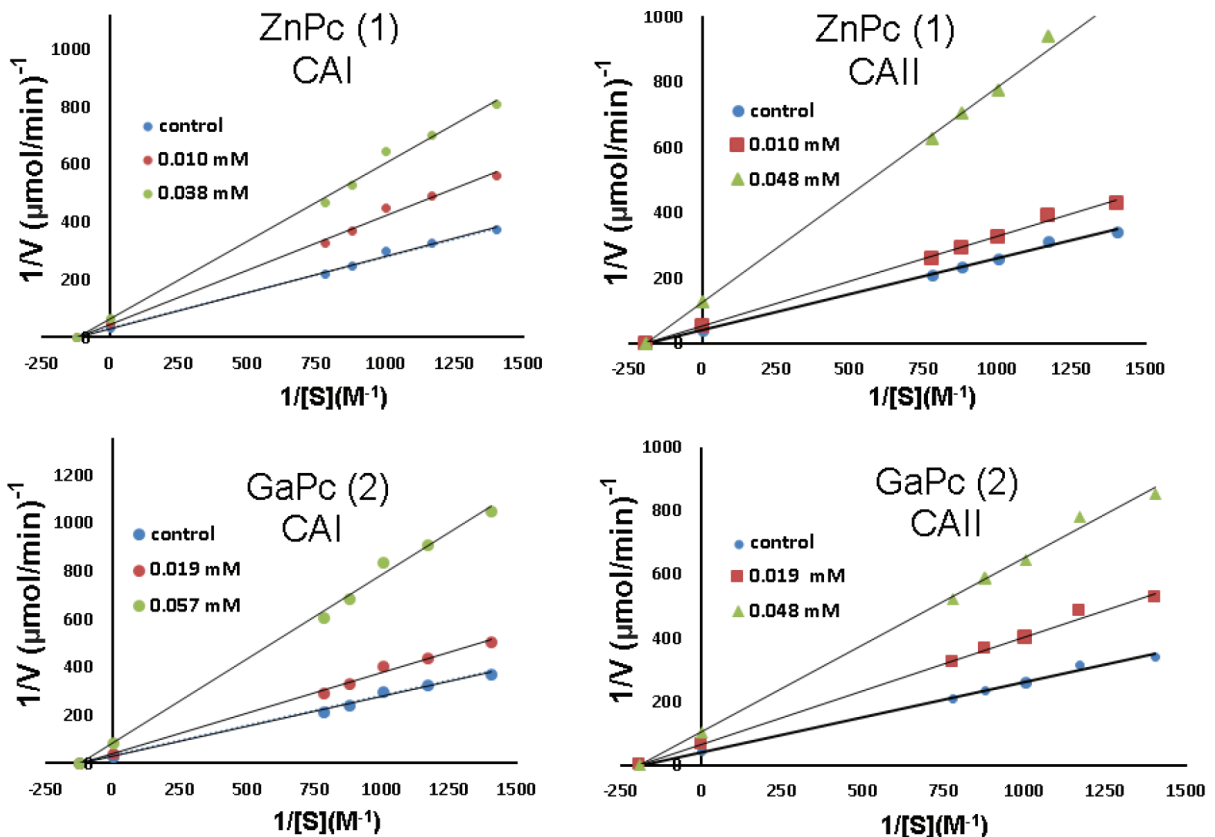


Figure 3. Lineweaver–Burk graphs of hCA I and hCA II isoenzymes for zinc and gallium phthalocyanine complexes (**1** and **2**).

the atomic diameter of the Zn metal is larger than Ga; thus, the Zn complex is bulkier than the Ga complex. Their different steric effects could change the inhibitory activity because of an entrance of the active site cavity and the van der Waals interactions with amino acid residues.

Acetazolamide (AAZ) is one of the best-known CAIs and is also used as a standard in CA assays [27]. Whereas complexes **1** and **2** showed much weaker inhibitory activity against hCA I and hCA II than AAZ (K_i of 250 nM and 12.1 nM against hCA I and hCA II, respectively) [28,29], they exhibited higher hCA I and II inhibitory activity than some synthesized compounds (K_i or IC_{50} values ranging between 75 μ M and 620 μ M against hCA I, between 126 μ M and 427 μ M against hCA II) reported as CAIs in the literature [30–33].

The sulphonamides (known as strong CAIs) bind in the deprotonated form to the catalytically critical Zn (II) ion in the enzyme active site [34,35], also contributing an extensive hydrogen bond and van der Waals interactions with amino acid residues of the enzyme active site, as reported in X-ray crystallographic studies of enzyme-inhibitor complexes [36]. We consider that the $-SO_3H$ moieties of the synthesized complexes can interact with Zn (II) ion and form the hydrogen bonds with amino acid residues in the enzyme active sites.

On the other hand, the in vitro inhibition effects of synthesized complexes on paraoxonase 1 (PON1) were investigated using paraoxon as a substrate. Both complex **1** and **2** inhibited PON1 (associated with HDL) with K_i of 0.37 μ M and 0.27 μ M, respectively, as noncompetitive inhibitors (Figure 4). These results demonstrated that complex **1** and **2** have a much stronger PON1 inhibitory activity than the reported PON1 inhibitors (K_i or IC_{50} values ranging between 35 μ M and 550 μ M) in the literature [37–39]. Besides, the changing metals and their atomic diameters have not shown a significant effect on PON1 inhibition.

3.1. Molecular docking studies

Docking calculations were carried out using the HEX 8.0.0 program [40]. This docking simulation program has allowed the calculation of drug candidate molecules for high atomic weight with a metal center. Docking calculation parameters are correlation type, compute device, FFT mode, and sampling method. These parameters are shape only, CPU, 3D, and range angles, respectively. Grid parameters are solution-100 and step size-(5.5, 5.5, 2.8). Docking simulations for investigated complexes were implemented against 4WR7, 5AML, and 1V04 target proteins representing hCA I, hCA II, and PON1 enzymes, respectively. 4WR7 is the crystal structure of human carbonic anhydrase isozyme I with 2,3,5,6-tetrafluoro-4-(propylthio) benzenesulfonamide. CA is an enzyme that catalyzes reversible carbon dioxide hydration. It is a metalloenzyme that ensures the regulation of acid-base balance and ion transport in all tissues and organs. It is known that

Table 1. K_i values of complex **1** and **2** against hCA I, hCA II and PON1.

Comp.	K_i (μ M) for hCA I	Inhibition type	K_i (μ M) for hCA II	Inhibition type	K_i (μ M) for PON1	Inhibition type
1	26.09	Noncompetitive	30.95	Noncompetitive	0.37	Noncompetitive
2	43.11	Noncompetitive	33.19	Noncompetitive	0.27	Noncompetitive

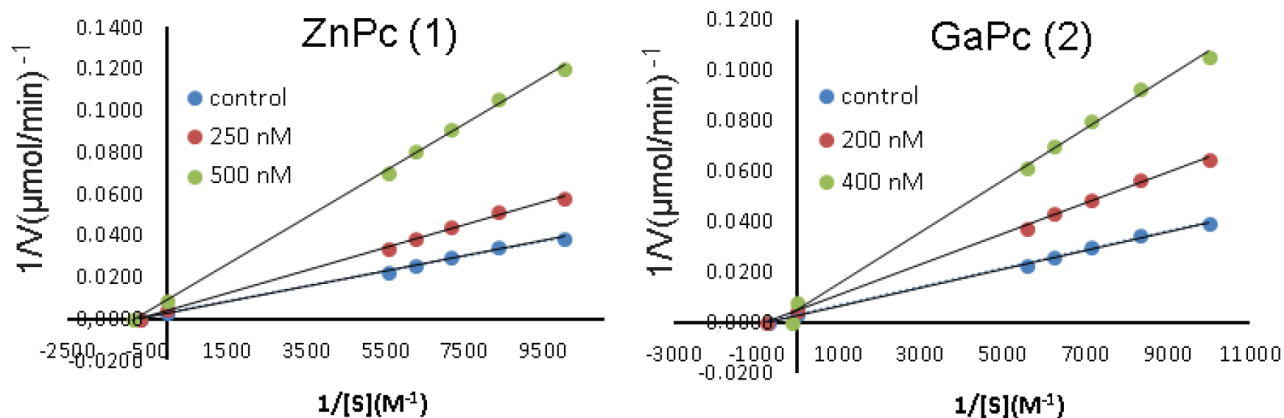


Figure 4. Lineweaver-Burk graphs of paraoxonase1 enzyme for complexes (**1** and **2**).

increased levels of different CAs are associated with various diseases such as epilepsy and cancer. Since the enthalpy and entropy distribution range of this protein is quite wide, it has a greater entropy contribution to the binding affinity during simulation than enthalpy [41]. 5AML is the three-dimensional structure of human carbonic anhydrase II in complex with 2-(but-2-yn-1-ylsulfamoyl)-4-sulfamoylbenzoic acid. The 5AML target protein has selectivity corresponding to some CA isoforms with medical applications. This protein has a high potential modulus as it contains aliphatic, alkenyl, aralkyl groups, and saccharin derivative substituents [42].

PON1 is a glycoprotein Ca^{2+} -dependent ester hydrolase, which is synthesized in the liver and is found in HDL in human serum, consisting of 355 amino acids [43]. PON1 is an enzyme with paraoxonase, arylesterase, and lactonase activities that can react with a wide variety of substrates [44]. The three-dimensional structure of a hybrid mammalian recombinant PON1 variant obtained by directed evolution (rePON1) was recently determined providing the first structural information about this hydrolase family, and this structure was named 1V04 [45]. The biological activity of synthesized zinc and gallium phthalocyanine complexes (1) and (2) against hCA I, hCA II, and PON enzymes was attempted to be elucidated by molecular simulation method. Secondary chemical interactions between the amino acid residues of the 4WR7, 5AML, and 1V04 target proteins and the complexes studied were also investigated. In the coupling studies, the estimated free energy of the binding values and the binding modes of the target proteins and metal complexes is given in Table 2 and Figure 5, respectively. According to the docking results in Table 2, the inhibition activities between the complexes and the target proteins, the gallium complex (2) is greater than the inhibition activity of the zinc complex (1). Gallium complex is located in the symmetry cavity of the 4WR7 target protein. Since the gallium complex contains chlorine atoms, it contains a halogen bond in the secondary chemical interaction type. The halogen bond occurs between the chlorine atom bound to the gallium metal and the Gln92 amino acid residue. Also, the gallium complex is in polar interaction with the target protein.

Table 2. The docking results between complexes (1) and (2) and the target proteins.

4WR7 (hCA I)	(1)	(2)
Binding energy (kcal/mol)	-4.20	-4.88
Type of interaction	H-bond	H-bond Halogen Polar
Binding site	His119	His94, Thr199 Gln92 Leu198
5AML (hCA II)	(1)	(2)
Binding energy (kcal/mol)	-4.07	-4.13
Type of interaction	H-bond	H-bond Halogen
Binding site	His94	His94, Thr199 His200, Asn62
1V04 (PON1)	(1)	(2)
Binding Energy (kcal/mol)	-5.25	-5.94
Type of interaction	H-bond Polar pi-pi	H-bond Halogen Polar pi-pi
Binding site	ASP54 GLU53, ASP54, ASN227 HIS115, TYR236	ASP269 HIS115, LEU240, LEU267, ILE291 HIS115, ASN168, ASP183, ASN224 HIS115, HIS285, PHE292

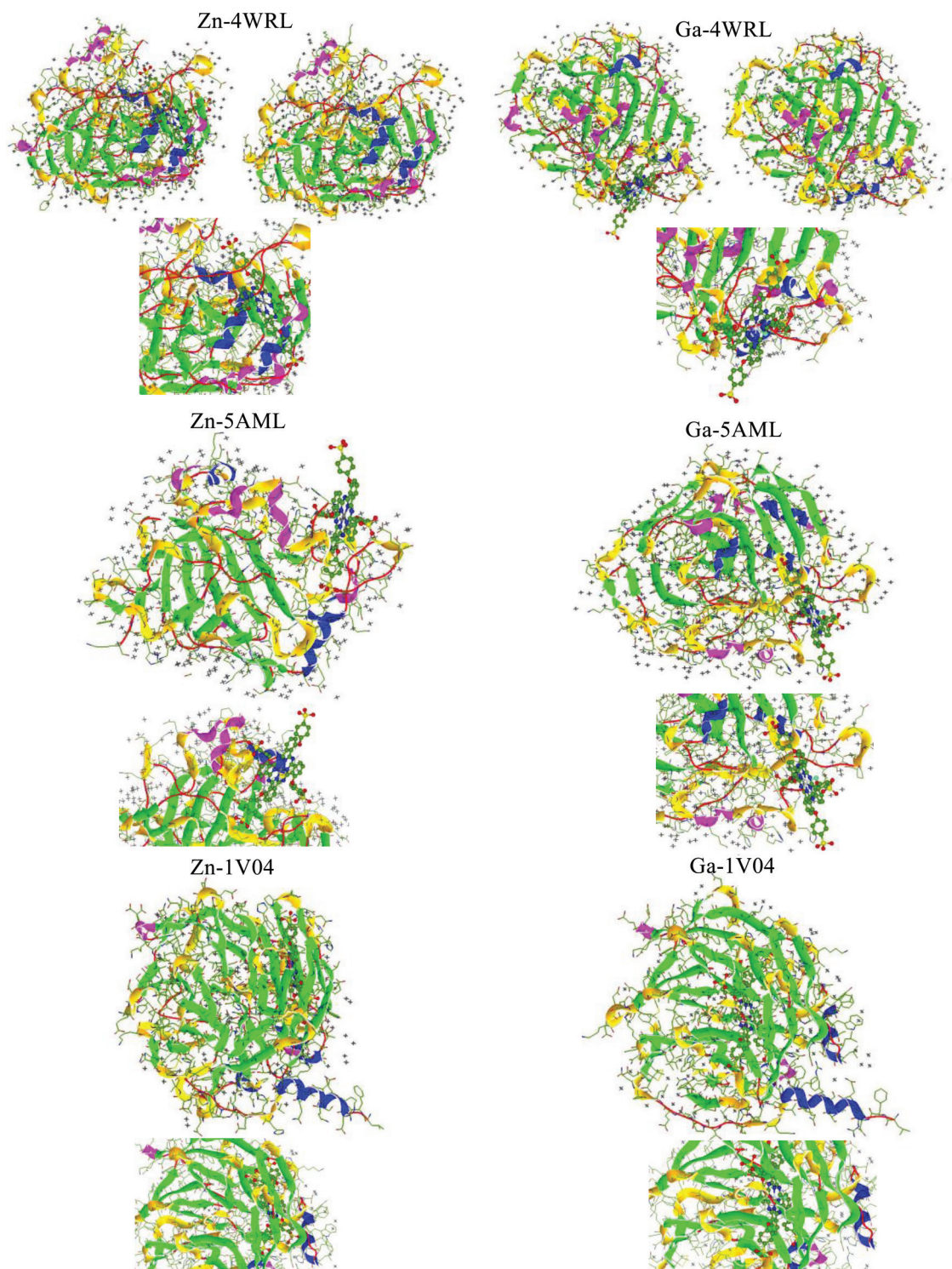


Figure 5. The binding modes between investigated phthalocyanine metal complexes and the determined target proteins.

The increase in the number of secondary chemical interactions between this complex and target proteins may have increased the estimated binding energy. It is clear from the results that in the gallium phthalocyanine complex there are two H-bonds between the His94 and Thr199 amino acid residues of the 4WR7 target protein. This is seen as an H-bond in the zinc complex. The H-bond appears between the zinc phthalocyanine complex and the His199 amino acid residue of

the 4WR7 target protein. Both metallophthalocyanine complexes show a similar trend with the 5AML target protein and the 4WR7 target protein. However, in contrast to the interaction of complexes with 5AML target protein, polar interaction is unlike any other.

Zinc and gallium complexes are in a stronger interaction with the 1V04 target protein, which represents the PON1 enzyme, compared to other enzymes. The types of secondary chemical interactions of the compounds with the 1V04 target protein are greater, as seen in Table 2. In the gallium metal-centered complex, unlike in the zinc complex, the halogen bond with the HIS115, LEU240, LEU267, and ILE291 amino acid residues draws attention. The binding energies obtained from the docking results show that the calculated energy values are in a trend parallel with enzyme activities.

As a result, simulation results tend to be similar to experimental inhibition activity. Docking studies are thought to be very important for understanding the chemical interaction mechanism in the inhibition effect.

4. Conclusion

In this paper, the investigation of carbonic anhydrase and paraoxonase enzyme inhibition properties of water-soluble sulfonated zinc and gallium phthalocyanines are reported for the first time. The results showed that complex **1** and **2** inhibited the cytosolic isoforms hCA I and hCA II (off-target cytosolic isoforms) in the micromolar range (K_i values of 26.09 μM and 43.11 μM for hCA I and 30.95 μM and 33.19 μM for hCA II, respectively). Moreover, they inhibited PON1 (associated with HDL) with K_i of 0.37 μM and 0.27 μM , respectively. The inhibition kinetics was analyzed by Lineweaver–Burk double reciprocal plots. The analysis revealed that complex **1** and **2** were noncompetitive inhibitors against PON1, hCA I, and hCA II. Whereas complex **1** and **2** showed moderate hCA I and hCA II inhibitory activity, they exhibited strong PON1 inhibitory activity. Furthermore, the changing metals (Zn and Ga) and their atomic diameters affected the CA inhibitory activity, while they did not show a significant effect on PON1. These complexes can be more preferable than other synthetic CA and PON inhibitors due to their high water solubility. Finally, the inhibition efficacy between zinc and gallium complexes and hCA I and hCA II enzymes has been studied in detail with molecular simulation, and experimental data and docking results are highly compatible.

Acknowledgment

This work was supported by the Research Fund of Balıkesir University (Research Project no: 2020/080) and Sakarya University of Applied Sciences.

References

- Çimen Y, Ermiş E, Dumludağ F, Özkaya AR, Salih B et al. Synthesis, characterization, electrochemistry and VOC sensing properties of novel ball-type dinuclear metallophthalocyanines. *Sensors and Actuators, B Chemistry* 2014; 202: 1137-1147.
- Yıldız B, Güzel E, Akyüz D, Arslan BS, Koca A et al. Unsymmetrically pyrazole-3-carboxylic acid substituted phthalocyanine-based photoanodes for use in water splitting photoelectrochemical and dye-sensitized solar cells. *Solar Energy* 2019; 191: 654-662.
- Korkut SE, Ocak H, Bilgin-Eran B, Güzeller D, Şener MK. Lyotropic liquid crystalline phthalocyanines containing 4-((S)-3,7-dimethyloctyloxy)phenoxy moieties. *Journal of Porphyrin and Phthalocyanines* 2017; 21: 16-23.
- Chino Y, Ohta K, Kimura M, Yasutake M. Discotic liquid crystals of transition metal complexes, 53 : synthesis and mesomorphism of phthalocyanines substituted by m-alkoxyphenylthio groups. *Journal of Porphyrin and Phthalocyanines* 2017; 21: 159-178.
- Güzel E, Orman EB, Köksoy B, Çelikbıçak Ö, Bulut M et al. Comparative electrochemistry and electrochromic application of novel binuclear double-decker rare earth metal phthalocyanines bearing 4-(hydroxyethyl)phenoxy moieties. *Journal of Electrochemical Society* 2019; 166: H438-H451.
- Wierchowski M, Łażewski D, Tardowski T, Grochocka M, Czajkowski R et al. Nanomolar photodynamic activity of porphyrins bearing 1,4,7-trioxanonyl and 2-methyl-5-nitroimidazole moieties against cancer cells. *Journal of Photochemistry and Photobiology B Biology* 2020; 202: 111703
- Sobotta L, Lijewski S, Długaszewska J, Nowicka J, Mielcarek J et al. Photodynamic inactivation of *Enterococcus faecalis* by conjugates of zinc(II) phthalocyanines with thymol and carvacrol loaded into lipid vesicles. *Inorganica Chimica Acta* 2019; 489: 180-190.
- Güzel E. Dual-purpose zinc and silicon complexes of 1,2,3-triazole group substituted phthalocyanine photosensitizers: synthesis and evaluation of photophysical, singlet oxygen generation, electrochemical and photovoltaic properties. *RSC Advances* 2019; 9: 10854-10864.
- Güzel E, Atsay A, Nalbantoglu S, Şaki N, Dogan AL et al. Synthesis, characterization and photodynamic activity of a new amphiphilic zinc phthalocyanine. *Dyes and Pigments* 2013; 97: 238-243.

10. Kurt Ö, Özçeşmeci İ, Sesalan BS, Koçak MB, The synthesis and investigation of binding properties of a new water soluble hexadeca zinc(ii) phthalocyanine with bovine serum albumin and DNA. *New Journal of Chemistry* 2015; 39 (7): 5767-5775.
11. Güzel E, Günsel A, Bilgiçli AT, Atmaca GY, Erdoğan A et al. Synthesis and photophysical properties of novel thiadiazole-substituted zinc (II), gallium (III) and silicon (IV) phthalocyanines for photodynamic therapy. *Inorganica Chimica Acta* 2017; 467: 169-176.
12. Dumoulin F, Durmuş M, Ahsen V, Nyokong T. Synthetic pathways to water-soluble phthalocyanines and close analogs. *Coordination Chemistry Reviews* 2010; 254: 2792-2847.
13. Feofanov A, Grichine A, Karmakova T, Kazachkina N, Pecherskih E et al. Chelation with metal is not essential for antitumor photodynamic activity of sulfonated phthalocyanines. *Photochemistry and Photobiology* 2007; 75: 527-533.
14. Güzel E, Yaşa Atmaca G, Erdoğan A, Koçak MB. Novel sulfonated hydrophilic indium(III) and gallium(III) phthalocyanine photosensitizers: preparation and investigation of photophysical properties. *Journal of Coordination Chemistry* 2017; 70: 2659-2670.
15. Topal M, Gülçin I. Rosmarinic acid: a potent carbonic anhydrase isoenzymes inhibitor. *Turkish Journal of Chemistry* 2014; 38: 894-902.
16. Mamedova G, Mahmudova A, Mamedov S, Erden Y, Taslimi P et al. Novel tribenzylaminobenzosulphonylimine based on their pyrazine and pyridazines: Synthesis, characterization, antidiabetic, anticancer, anticholinergic, and molecular docking studies. *Bioorganic Chemistry* 2019; 93: 103313.
17. Taslimi P, Türkan F, Cetin A, Burhan H, Karaman M et al. Pyrazole[3,4-d]pyridazine derivatives: Molecular docking and explore of acetylcholinesterase and carbonic anhydrase enzymes inhibitors as anticholinergics potentials. *Bioorganic Chemistry* 2019; 92: 103213.
18. Erdemir F, Celepci DB, Aktaş A, Gök Y, Kaya R et al. Novel 2-aminopyridine liganded Pd(II) N-heterocyclic carbene complexes: Synthesis, characterization, crystal structure and bioactivity properties. *Bioorganic Chemistry* 2019; 91: 103134.
19. Arslan T, Çakır N, Keleş T, Biyiklioglu Z, Senturk M. Triazole substituted metal-free, metallo-phthalocyanines and their water soluble derivatives as potential cholinesterases inhibitors: Design, synthesis and in vitro inhibition study. *Bioorganic Chemistry* 2019; 90: 103100.
20. Arslan T, Biyiklioglu Z, Şentürk M. The synthesis of axially disubstituted silicon phthalocyanines, their quaternized derivatives and first inhibitory effect on human cytosolic carbonic anhydrase isozymes hCA I and II. *RSC Advances* 2018; 8: 10172-10178.
21. Günsel A, Bilgiçli AT, Barut B, Taslimi P, Özel A et al. Synthesis of water soluble tetra-substituted phthalocyanines: Investigation of DNA cleavage, cytotoxic effects and metabolic enzymes inhibition. *Journal of Molecular Structure* 2020; 1214: 128210.
22. Mentеше E, Baltaş N, Bekircan O. Synthesis and kinetics studies of *N'*-(2-(3,5-disubstituted-4 H -1,2,4-triazol-4-yl)acetyl)-6/7/8-substituted-2-oxo-2 H -chromen-3-carbohydrazide derivatives as potent antidiabetic agents. *Archive der Pharmazie (Weinheim)* 2019; 352: 1900227.
23. Güzel E, Koca A, Koçak MB. Anionic water-soluble sulfonated phthalocyanines: microwave-assisted synthesis, aggregation behaviours, electrochemical and in-situ spectroelectrochemical characterisation. *Supramolecular Chemistry* 2017; 29: 536-546.
24. Güzel E, Yarasir MN, Özkaya AR. Low symmetry solitaire- and trans-functional porphyrazine/phthalocyanine hybrid complexes: Synthesis, isolation, characterization, and electrochemical and in-situ spectroelectrochemical properties. *Synthetic Metals* 2020; 262: 116331.
25. Zheng X, Wang Y, Hu J, Yang G, Guo Z et al. Octamethyl-substituted Pd(ii) phthalocyanine with long carrier lifetime as a dopant-free hole selective material for performance enhancement of perovskite solar cells. *Journal of Material Chemistry A* 2017; 5: 24416-24424.
26. Güzel E, Koca A, Gül A, Koçak MB. Microwave-assisted synthesis, electrochemistry and spectroelectrochemistry of amphiphilic phthalocyanines. *Synthetic Metals* 2015; 199: 372-380.
27. Zengin Kurt B, Sonmez F, Ozturk D, Akdemir A, Angeli A et al. Synthesis of coumarin-sulfonamide derivatives and determination of their cytotoxicity, carbonic anhydrase inhibitory and molecular docking studies. *European Journal of Medicinal Chemistry* 2019; 183: 111702.
28. Zengin Kurt B, Sonmez F, Durdagi S, Aksoydan B, Ekhteiari SR et al. Synthesis, biological activity and multiscale molecular modeling studies for coumaryl-carboxamide derivatives as selective carbonic anhydrase IX inhibitors. *Journal of Enzyme Inhibition Medicinal Chemistry* 2017; 32: 1042-1052.
29. Kurt BZ, Dag A, Doğan B, Durdagi S, Angeli A et al. Synthesis, biological activity and multiscale molecular modeling studies of bis-coumarins as selective carbonic anhydrase IX and XII inhibitors with effective cytotoxicity against hepatocellular carcinoma. *Bioorganic Chemistry* 2019; 87: 838-850.
30. Rifati-Nixha A, Arslan M, Gençer N, Çıkrıkçı K, Gökçe B et al. Synthesis of carbazole bearing pyridopyrimidine-substituted sulfonamide derivatives and studies their carbonic anhydrase enzyme activity. *Journal of Biochemical and Molecular Toxicology* 2019; 33 (6): e22306.
31. Karlık Ö, Gençer N, Karataş MO, Ergün A, Çıkrıkçı K et al. Microwave-assisted synthesis of 1-substituted-1 H -benzimidazolium salts: Non-competitive inhibition of human carbonic anhydrase I and II. *Archive der Pharmazie (Weinheim)* 2019; 352: 1800325.

32. Atahan A, Gencer N, Bilen C, Yavuz E, Genc H et al. Synthesis, biological activity and structure-activity relationship of novel diphenylurea derivatives containing tetrahydroquinoline as carbonic anhydrase I and II inhibitors. *Chemistry Select* 2018; 3: 529-534.
33. Kurt BZ, Sonmez F, Gokce B, Ergun A, Gencer N et al. In vitro inhibition effects on erythrocyte carbonic anhydrase I and II and structure-activity relationships of cumarylthiazole derivatives. *Russian Journal of Bioorganic Chemistry* 2016; 42: 506-511.
34. Kurt BZ, Sönmez F, Bilen Ç, Ergun A, Gençer N, Arslan O et al. Synthesis, antioxidant and carbonic anhydrase I and II inhibitory activities of novel sulphonamide-substituted coumarylthiazole derivatives. *Journal of Enzyme Inhibition Medicinal Chemistry* 2016; 31: 991-998.
35. Congiu C, Onnis V, Balboni G, Supuran CT. Synthesis and carbonic anhydrase I, II, IX and XII inhibition studies of 4-N,N-disubstituted sulfanilamides incorporating 4,4,4-trifluoro-3-oxo-but-1-enyl, phenacylthiourea and imidazol-2(3H)-one/thione moieties. *Bioorganic Medicinal Chemistry Letters* 2014; 24: 1776-1779.
36. D'Ambrosio K, Smaine FZ, Carta F, De Simone G, Winum JY et al. Development of potent carbonic anhydrase inhibitors incorporating both sulfonamide and sulfamide groups. *Journal of Medicinal Chemistry* 2012; 55: 6776-6783.
37. Gökçe B, Sarıoğlu N, Gençer N, Arslan O. Association of human serum paraoxonase-1 with some respiratory drugs. *Journal of Biochemical and Molecular Toxicology* 2019; 33 (12): e22407.
38. Karataş MO, Çalgın G, Alici B, Gökçe B, Gençer N et al. Inhibition of paraoxonase 1 by coumarin-substituted N-heterocyclic carbene silver(I), ruthenium(II) and palladium(II) complexes. *Applied Organometallic Chemistry* 2019; 33 (10): e5130.
39. Karataş MO, Uslu H, Alici B, Gökçe B, Gencer N et al. Functionalized imidazolium and benzimidazolium salts as paraoxonase 1 inhibitors: Synthesis, characterization and molecular docking studies. *Bioorganic Medicinal Chemistry* 2016; 24: 1392-1401.
40. Ritchie DW. Hex 8.0.0 User Manual; INRIA Nancy Grand Est, LORIA, Team Orpailleur; 1996-2013.
41. Zubriene A, Smirnoviene J, Smirnov A, Morkunaite V, Michailoviene V et al. Intrinsic thermodynamics of 4-substituted-2,3,5,6-tetrafluorobenzenesulfonamide binding to carbonic anhydrases by isothermal titration calorimetry. *Biophysical Chemistry* 2015; 205: 51-65.
42. Ivanova J, Leitans J, Tanc M, Kazaks A, Zalubovskis R et al. X-ray crystallography-promoted drug design of carbonic anhydrase inhibitors. *Chemical Communication* 2015; 51: 7108-7111.
43. Sorenson RC, Aviram M, Bisgaier CL, Billecke S, Hsu C et al. Properties of the retained N-terminal hydrophobic leader sequence in human serum paraoxonase/arylesterase. *Chemico-Biological Interactions* 1999; 119-120: 243-249.
44. Rodrigo L, Hernández AF, López-Caballero JJ, Gil F, Pla A. Immunohistochemical evidence for the expression and induction of paraoxonase in rat liver, kidney, lung and brain tissue. Implications for its physiological role. *Chemico-Biological Interaction* 2001; 137: 123-137.
45. Harel M, Aharoni A, Gaidukov L, Brumshtein B, Khersonsky O et al. Structure and evolution of the serum paraoxonase family of detoxifying and anti-atherosclerotic enzymes. *Nature Structural & Molecular Biology* 2004; 11: 412-419.

SUPPORTING INFORMATION

1. Materials

All reagents and solvents were of reagent grade quality and were obtained from commercial suppliers. The homogeneity of the products was tested in each step by TLC. The solvents were stored over molecular sieves. All solvents were dried and purified.

2. Equipment

IR spectra were recorded on a Thermo Scientific iS10 FT-IR (ATR sampling accessory) spectrophotometer and electronic spectra on a Shimadzu UV-2450 UV-vis spectrophotometer. $^1\text{H-NMR}$ and $^{13}\text{C-NMR}$ spectra were recorded on Agilent VNMRs 300 MHz and the spectrum was referenced internally by using the residual solvent resonances; chemical shifts were reported relative to Me_4Si as an internal standard. Mass spectra were measured on a Micromass Quatro LC/ULTIMA LC-MS/MS spectrometer and MALDI-MS of complexes were obtained in dihydroxybenzoic acid as MALDI matrix using nitrogen laser accumulating 50 laser shots using Bruker Microflex LT MALDI-TOF mass spectrometer, Bremen, Germany.

3. Biological activity assays

Preparation of hemolysate and purification from red blood cells

Blood samples (25 mL) from healthy human volunteers were collected. They were centrifuged at $1000 \times g$ for 20 min at 4°C and the supernatant was removed. The packed erythrocytes were washed three times with 0.9% NaCl and then hemolyzed in cold water. The pH of the hemolysate was adjusted to 8.5 with a solid Tris-base. Twenty-five milliliters of hemolysate were applied to an affinity column containing Sepharose 4B-ethylene diamine-4-isothiocyanato-benzenesulfonamide [1]. CA isozymes were then eluted with 0.1 M NaCl / 25 mM Na_2HPO_4 (pH 6.3) and 0.1 M CH_3COONa / 0.5 M NaClO_4 (pH 5.6), which recovered hCA I and II, respectively.

Hydratase activity assay

CA activity was measured with the Maren method based on the determination of the time required for the pH to decrease from 10.0 to 7.4 due to CO_2 hydration. The assay solution was 0.5 M Na_2CO_3 / 0.1 M NaHCO_3 (pH 10.0); and phenol red was added as the pH indicator. CO_2 -hydratase activity (enzyme units [EU]) was calculated by using the equation $t_0 - tc / tc$, where t_0 and tc are the times for pH change of the nonenzymatic and the enzymatic reactions, respectively. For the inhibition studies of complexes, different concentrations of these compounds were added to the enzyme. Activity % values of CA for different concentrations of each compound were determined by regression analysis using Microsoft Office 2000 Excel. CA enzyme activity without a sample was accepted as 100% activity. For the compounds having an inhibition effect, the inhibitor concentration causing up to 50% inhibition (IC_{50} values) was determined from the graphs.

Esterase activity assay

CA activity was assayed by following the change in absorbance at 348 nm of 4-nitrophenyl-acetate (NPA) to 4-nitrophenylate ion over a period of 3 min at 25°C using a spectrophotometer (Biotek Power Wave XS) according to the method described in the literature [2]. The inhibitory effects of zinc and gallium complexes (**1** and **2**) on enzyme activities were tested under in vitro conditions; K_i values were calculated from Lineweaver–Burk [3] graphs.

Purification of paraoxonase from human serum by hydrophobic interaction chromatography

Human serum was isolated from 40 mL of fresh human blood and added into a dry tube. The blood samples were centrifuged at 3000 rpm for 15 min and the serum was removed. Firstly, serum paraoxonase was obtained via ammonium sulphate precipitation (60%–80%). The precipitate was accumulated by centrifugation at 15,000 rpm for 40 min and dissolved in 100 mM Tris–HCl buffer (pH 8.0). Then, for the purification of human serum paraoxonase, we used hydrophobic interaction chromatographic gel-(Sepharose 4B, L-tyrosine 1-naphthylamine) [4]. The column was equilibrated with 0.1 M of a Na_2HPO_4 buffer (pH 8.00), including 1 M ammonium sulphate. The paraoxonase was eluted with an ammonium sulphate gradient using 0.1 M Na_2HPO_4 buffer with and without ammonium sulphate (pH 8.00).

Paraoxonase enzyme assay

Paraoxonase enzyme activity was quantified spectrophotometrically using paraoxon substrate by the method identified in Gan et al. [5]. The reaction was determined for 1 min at 37°C via the appearance of *p*-nitrophenol at 412 nm in a Biotek automated recording spectrophotometer. The final substrate concentration during enzyme assay was 2 mM, and all rates were measured in duplicate and corrected for the nonenzymatic hydrolysis. The paraoxonase enzyme unit was defined as the quantity of enzyme that hydrolyses 1 μmol of *p*-nitrophenol. A molar extinction coefficient (ϵ) of $17,100 \text{ M}^{-1}\text{cm}^{-1}$ for *p*-nitrophenol at pH 8.0 in 100 mM Tris–base buffer was used for the calculation.

In vitro kinetic studies

For the kinetic studies of synthesized complexes, different concentrations were added to the enzyme activity. Paraoxonase activity with compounds was assayed by following the hydration of paraoxon. Activity % values of paraoxonase for five or more different concentrations of each complex were determined by regression analysis using Microsoft Office 2010 Excel. Control enzyme activity without the complex was 100% and the activity of each compound increased the ratio. For the compounds having an inhibition effect, the inhibitor concentration causing up to 50% inhibition (IC_{50} values) was determined from the graphs.

Total protein determination

Absorbance at 280 nm was used to monitor the protein in the column effluents and ammonium sulphate precipitation. Quantitative protein determination was achieved by absorbance measurements at 595 nm according to Bradford [6] with bovine serum albumin as a standard.

SDS polyacrylamide gel electrophoresis

After purification of human paraoxonase1 (hPON1), sodium dodecyl sulphate polyacrylamide gel electrophoresis (SDS-PAGE) was applied in two different acrylamide concentrations, 10% and 3%, for the running and stacking gel, respectively, consisting of 0.1% SDS. A 20 mg sample was added to the electrophoresis composition. The gel was kept overnight in 0.1% Coomassie Brilliant Blue R-250 in 50% methanol and 10% acetic acid, then detained by fast changing the same solvent, without dye. The electrophoretic figure was photographed; an image of the gel is shown in Figure S1.

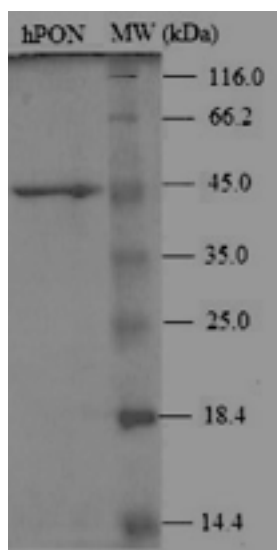


Figure S1. SDS-PAGE of human serum paraoxonase1. The pooled fractions from hydrophobic interaction chromatographic were analyzed by SDS-PAGE (12% and 3%) and revealed by Coomassie Blue staining. Experimental conditions were as described in the method. Lane 1 contained 5 μ L of various molecular mass standards: 3-galactosidase (116.0), bovine serum albumin (66.2), ovalbumin (45.0), lactate dehydrogenase (35.0), restriction endonuclease (25.0), 3-lactoglobulin (18.4), lysozyme (14.4). Only one protein-staining band was detectable on Line 2.

4. Preparation of the phthalocyanine complexes

General procedures for phthalocyanine complexes

Reaction: A mixture of 4-(2,3-dicyanophenoxy)benzenesulfonic acid (0.100 g, 0.333 mmol), 0.110 mmol anhydrous metal salts ($ZnCl_2$, 0.020 g, $GaCl_3$, 0.015 g), and a catalytic amount of DBU (1,8-diazabicyclo[5.4.0]undec-7-ene) in n-pentanol (2 cm^3) was irradiated with a microwave at 145 $^{\circ}C$ in a sealed glass tube for 25 min under a nitrogen atmosphere. **Work up:** After cooling to room temperature, the green mixture was cooled, precipitated by adding hexane, and filtered. **Purification:** After being washed with cold ethanol, chloroform, and then with acetone several times, the deep blue-green product was dissolved in HCl solution (50 mL, 0.8 M), reprecipitated with an excess of acetone, and dried in vacuo at 100 $^{\circ}C$. **Solubility:** Highly soluble in water and moderately soluble in DMF and DMSO.

Zinc phthalocyanine (1): Yield: 0.065 g, 61%, FTIR, cm^{-1} 3429 (m, SO_3H), 3071 (w, C-H), 1583 (m, Ar), 1216 (s, R-O-Ar), 1209 (m, S=O asym.st), 1122 (s, SO_3H), 1032 (s, S=O sym. st.). UV-vis λ_{max} (nm) DMSO: 695, 329; 1H -NMR (300 MHz, $DMSO-d_6$): δ , ppm 9.12–8.44 (4H, Pc-Ar-H) 7.58–7.46 (16H, m, Pc-Ar-H and Ar-H), 7.08–7.00 (8H, m, Ar-H).

MALDI-TOF-MS m/z : 1328 $[M + Na + K]^+$. Elemental analysis, calcd. for $C_{58}H_{32}N_6O_{16}S_4Zn$ %: C, 55.17; H, 2.55; N, 6.66; O, 20.28; S, 10.16; found C, 56.98; H, 2.72; N, 6.16. m.p. > 200 °C.

Gallium phthalocyanine (2): Yield: 0.047 g. 44%, FT-IR (ν_{max}/cm^{-1}): 3071, 3043 (w, C-H), 1584 (m, Ar), 1222 (s, R-O-Ar), 1179 (m, S=O asym.st), 1119 (s, SO_3H), 1029 (s, S=O sym. st.). UV-vis λ_{max} (nm) DMSO: 711, 639, 344. 1H -NMR (300 MHz, DMSO- d_6): δ , ppm 1H -NMR (300 MHz, DMSO- d_6): δ , ppm 9.47–8.84 (4H, Pc-Ar-H) 8.46–7.28 (16H, m, Pc-Ar-H and Ar-H), 7.16–7.00 (8H, m, Ar-H). MALDI-TOF-MS m/z : 1426 $[M-Cl + matrix]^+$. Elemental analysis, anal. calcd. for $C_{57}H_{32}N_8O_{16}S_4GaCl$ %: C, 51.49; H, 2.47; Cl, 2.71; Ga, 5.34; N, 8.58; O, 19.60; S, 9.82; found C, 51.98; H, 2.82; N, 8.16. m.p. > 200 °C.

5. The IC_{50} graphs of complex 1 and 2 for hCA I, hCA II, and PON1

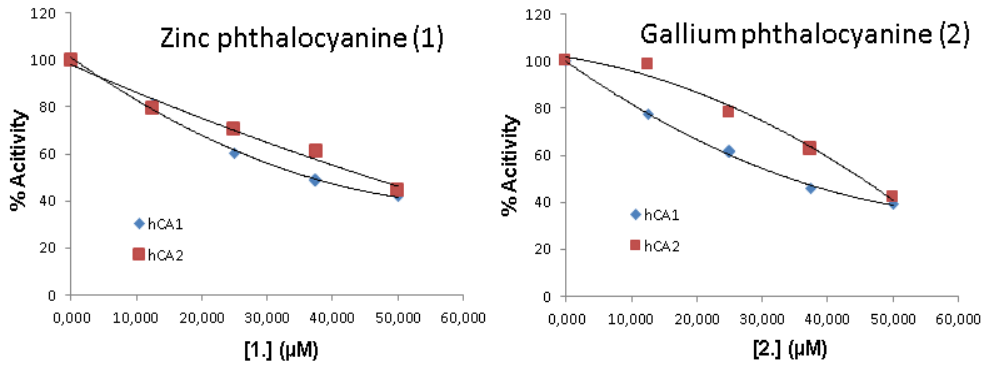


Figure S2. IC_{50} graphs of complexes (1 and 2) for hCA I and hCA II isoenzymes (hydratase activity).

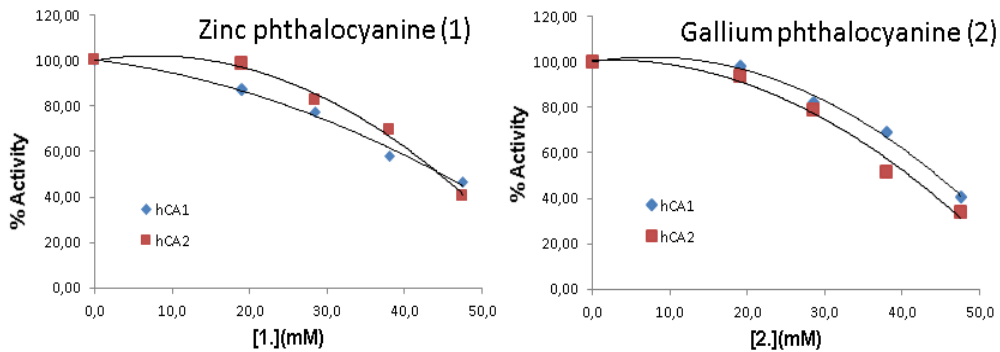


Figure S3. IC_{50} graphs of complexes (1 and 2) for hCA I and hCA II isoenzymes (esterase activity).

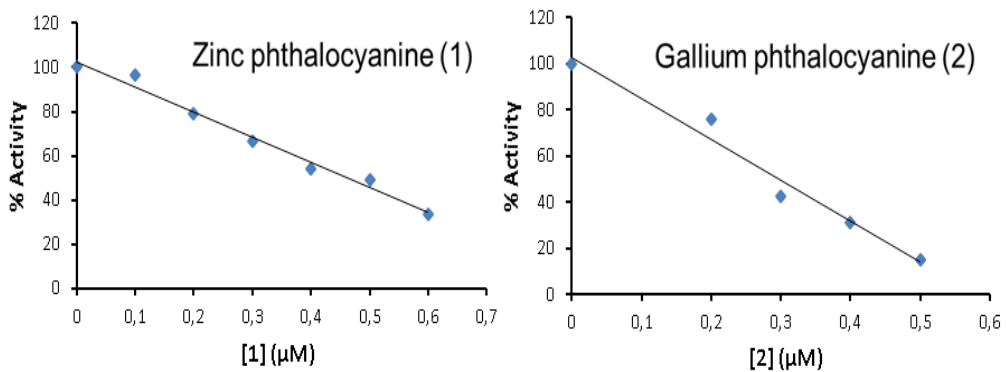


Figure S4. IC_{50} graphs of complexes (1 and 2) for paraoxonase1.

References

1. Bozdag M, Isik S, Beyaztas S, Arslan O, Supuran CT. Synthesis of a novel affinity gel for the purification of carbonic anhydrases. *Journal of Enzyme Inhibition Medicinal Chemistry* 2015; 30: 240-244.
2. Jacob A, Verpoorte, Suchinta Mehta JTE. Esterase Activities of Human Carbonic Anhydrases B and C. *Journal of Biological Chemistry* 1967; 242: 4221-4229.
3. Burk HL and D. The Determination of Enzyme Dissociation Constants. *Journal of American Chemical Society* 1934; 56: 658-666.
4. Sinan S, Kockar F, Arslan O. Novel purification strategy for human PON1 and inhibition of the activity by cephalosporin and aminoglikozide derived antibiotics. *Biochimie* 2006; 88: 565-574.
5. Chen X, Wang C, Xu J, Wang F, Jiang Y et al. Purification and Characterization of a Novel Lipase from Antarctic Krill. *Journal of Ocean University of China* 2020; 19: 209-215.
6. McRorie RA, Turner RB, Bradford MM, Williams WL. Acrolysin, the aminoproteinase catalyzing the initial conversion of proacrosin to acrosin in mammalian fertilization. *Biochemical and Biophysical Research Communications* 1976; 71: 492-498.